Circ J 2004; **68**: 376–382

Effects of Aldosterone Receptor Antagonist and Angiotensin II Type I Receptor Blocker on Cardiac Transcriptional Factors and mRNA Expression in Rats With Myocardial Infarction

Ryo Matsumoto, MD; Minoru Yoshiyama, MD; Takashi Omura, MD; Shokei Kim, MD*; Yasuhiro Nakamura, MD; Yasukatsu Izumi, MD; Kaname Akioka, MD; Hiroshi Iwao, MD*; Kazuhide Takeuchi, MD; Junichi Yoshikawa, MD

Background Because the effects of an aldosterone receptor antagonist on transcriptional factors and mRNA expression have not been fully examined in myocardial infarction (MI), the present study examined the effects of spironolactone (SPIRO) and candesartan cilexitil (CAN) on activation of activator protein-1 (AP-1), nuclear factor-κB (NF-κB) and mRNA expression in the non-ischemic myocardium after MI.

Methods and Results MI was induced by ligation of the coronary artery in Wistar rats, which were separated into (1) vehicle-treated group, (2) CAN-treated group (10mg/kg per day), (3) SPIRO-treated group (100mg/kg per day) and (4) CAN+SPIRO-treated group. The activity of both AP-1 and NF-κB was significantly increased at 4 weeks after MI. CAN or SPIRO significantly prevented the cardiac remodeling and activity of AP-1 and NF-κB. Furthermore, CAN+SPIRO prevented the cardiac remodeling and activation of AP-1 and NF-κB, compared with CAN or SPIRO alone. Myocardial atrial natriuretic peptide, brain natriuretic peptide, collagen I and III mRNAs were enhanced by MI, and CAN or SPIRO alone significantly reduced the mRNAs. CAN+SPIRO significantly prevented these mRNAs, compared with CAN or SPIRO alone.

Conclusions Both aldosterone and angiotensin II are involved in the myocardial transcriptional activation of AP-1, NF-κB and the cardiac remodeling-related mRNAs. The combination of CAN and SPIRO may be a potent therapeutic strategy for preventing cardiac remodeling after MI. (*Circ J* 2004; **68**: 376–382)

Key Words: Activator protein-1; Angiotensin II; Cardiac remodeling; Nuclear factor-κB; Spironolactone

After myocardial infarction (MI), there is acute phase (termed 'infarct expansion') and second phase cardiac remodeling. Infarct expansion is a structural rearrangement, such as thinning of the infarcted myocardium and dilatation of the ventricular cavity[1,2] that is histologically characterized by myocardial cell damage, inflammatory change and the expression of extracellular matrix components. Moreover, the second phase, which is characterized by myocardial hypertrophy and ventricular dilatation in the non-infarcted region, begins after stabilization of the infarct scar[3] Infarct expansion, ventricular dilatation and fibrosis of viable myocardium are all maladaptive processes that contribute to left ventricular (LV) dysfunction and progression to heart failure. Thus remodeling not only compensates for the deficiency in function of the infarcted region[4] but may also be related to the accelerated intracellular signal transduction system, through growth factors and/or neurotransmitters, after MI.

Accumulating evidence shows that the renin–angiotensin system plays an important role in modulating cardiac remodeling after MI. Angiotensin-converting enzyme inhibitor (ACEI)[5,6] and angiotensin II type I receptor blockers (ARB)[7,8] are known to improve the quality of life and decrease the mortality and morbidity of patients with MI. These drugs have been shown to prevent chamber dilatation, dysfunction, and hypertrophy in the non-infarcted myocardium by suppressing the increased mRNA expression of atrial natriuretic peptide (ANP), α-skeletal actin and β-myosin heavy chain, and collagen types I and III[9] These responses require increased activity of transcriptional factors, which are considered to be important for cell growth, differentiation and apoptosis. Recently, it was shown that angiotensin II (Ang II) activates activator protein-1 (AP-1) in cultured cardiomyocytes or rat hearts after MI, which suggests that the AP-1 activated by Ang II may be important in the process of cardiac hypertrophy[10] On the other hand, nuclear factor κB (NF-κB) plays a central role in the expression of many genes involved in the inflammatory and immune response[11] It is well known that MI activates local and systemic inflammatory responses that are regulated by cytokines[12,13] We have previously reported that the activation of non-infarcted myocardial AP-1 and NF-κB was reduced by ACEI and ARB[14] which suggests that myocardial AP-1 and NF-κB may be important transcriptional factors for the response to ventricular remodeling after MI.

Furthermore, in the Randomized Aldactone Evaluation Study (RALES), the mineralocorticoid receptor antagonist,

(Received October 23, 2003; revised manuscript received December 25, 2003; accepted January 16, 2004)

*Departments of Internal Medicine and Cardiology, and *Pharmacology, Osaka City University Medical School, Osaka, Japan*
Mailing address: Minoru Yoshiyama, Department of Internal Medicine and Cardiology, Osaka City University Medical School, 1-4-3 Asahimachi, Abeno-ku, Osaka 545-8585, Japan. E-mail: yoshiyama@med.osaka-cu.ac.jp

spironolactone, was shown to reduce mortality in patients with congestive heart failure, and the beneficial outcome was shown to be associated with the suppression of cardiac collagen synthesis[15] However, the effects of the inhibition of aldosterone on myocardial AP-1 and NF-κB after MI have not been examined in vivo. The purpose of this study was to elucidate the effects of spironolactone, with or without ARB, on myocardial AP-1 and NF-κB and the expression of remodeling-related mRNA in non-infarcted myocardium after MI.

Methods

Experimental Animals and Protocol

Male Wistar rats weighing 290–310g were purchased from Clea Japan, Inc (Osaka, Japan). MI was produced by ligation of the left coronary artery as previously described[16] The same surgical procedure was performed in a sham group of rats except that the suture around the coronary artery was not tied. Candesartan cilexitil (CAN), an Ang II type 1 (AT_1) receptor antagonist, was provided by Takeda Co Ltd (Osaka, Japan). Spironolactone (SPIRO), an aldosterone receptor antagonist, was purchased from Sigma Chemical Industries Ltd (St Louis, MI, USA). Rats that survived after coronary ligation were randomly divided into 4 groups and treated with (1) vehicle (0.5% carboxymethylcellulose solution), (2) CAN (10mg/kg per day)[9] (3) SPIRO (100mg/kg per day)[17] or (4) the combination of 10mg/kg per day of CAN and 100mg/kg per day of SPIRO. All drugs were given to the MI rats by gastric gavage once daily for 4 weeks after MI.

Doppler-Echocardiographic Studies and Physiological Studies

Transthoracic echocardiograph studies were performed as previously described in detail[9,18] In brief, rats were lightly anesthetized with an intraperitoneal injection of ketamine HCl and xylazine. Echocardiograms were recorded using an echocardiographic system equipped with a 12.0-MHz phased-array transducer (SONOS 5500; Philips Medical System, Best, The Netherlands). Two-dimensional short-axis views of the left ventricle and M-mode tracings were recorded through the anterior and posterior LV walls at the papillary muscle level to measure the LV end-diastolic dimension (LVDd). LV ejection fraction (LVEF) and LV end-diastolic volume (LVEDV) by modified Simpson's method, which uses a 4-chamber view. Pulse-wave Doppler spectra (E and A waves velocity) of mitral inflow were recorded from the apical 4-chamber view, with the sample volume placed near the tips of the mitral leaflets. All Doppler spectra were recorded on paper at 100mm/s and analyzed off-line.

The method of measuring the hemodynamics has been described in detail[16] In brief, LV pressure was recorded by inserting a polyethylene catheter (0.58-mm internal diameter, PE-50) into the right carotid artery and advancing it into the LV. Water-filled catheters were connected to the tubing connected to a water-filled pressure transducer. The pressures were recorded on a physiological recorder while the rats were breathing spontaneously. LV end-diastolic pressure (LVEDP) was obtained by averaging the values for 10beats. Myocardial infarct size was measured as previously described[16] Rats with an infarct <30% were excluded from analysis because they did not show typical LV remodeling. After determination of infarct size, the heart was immediately excised and the septal myocardium was dissected as the non-infarcted myocardium. The specimens were immediately frozen and stored at –80°C until use.

Electrophoretic Mobility Shift Assays

LV tissue was immediately washed in precooled phosphate buffered salin (pH 7.4) containing 2.5mmol/L EDTA, 2mmol/L glycerophosphate, 10mmol/L NaF and 1mmol/L Na_3VO_4 and homogenized with a Dounce homogenizer in 1ml of cold buffer A (10mmol/L HEPES (pH 7.9), 10mmol/L KCl, 0.1mmol/L EDTA, 0.1mmol/L EGTA, 1.5mmol/L $MgCl_2$, 10mmol/L NaF, 1mmol/L Na_3VO_4, 0.5mmol/L phenylmethylsulfonyl fluoride (PMSF), 1mmol/L dithiothreitol (DTT), 20mmol/L glycerophosphate, 60μg/ml aprotinin and 2μg/ml leupeptin). The tissue homogenates were transferred into Eppendorf tubes and the cells were allowed to swell on ice for 15min, after which 62.5μl of 10% Nonidet P-40 was added and the tubes were vigorously vortex-mixed for 10s. The nuclear fractions were precipitated by centrifugation at 3,500G for 10min at 4°C and then resuspended in 150μl of cold buffer C (20mmol/L HEPES (pH 7.9), 0.4mol/L NaCl, 1mmol/L EDTA, 1mmol/L EGTA, 1.5mmol/L $MgCl_2$, 20% glycerol, 10mmol/L NaF, 1mmol/L Na_3VO_4, 0.5mmol/L PMSF, 0.2mmol/L DTT, 20mmol/L glycerophosphate, 60μg/ml aprotinin and 2μmg/ml leupeptin); the tubes were rocked for 10min at 4°C. Following centrifugation at 10,000G for 10min at 4°C, the supernatants containing nuclear protein were collected and stored at –80°C until use.

The sequence of the double-stranded oligonucleotides used in the present study was as follows:

consensus AP-1, 5'-CGCTTGATGACTCAGCCGGAA-3'
consensus NF-κB, 5'-AGTTGAGGGGACTTTCCCAGGC-3'

The oligonucleotide probes were labeled with (γ-^{32}P) ATP at the 5' end, using T_4 polynucleotide kinase, and the labeled probes were purified by chromatography on a Bio-Spin column (Bio-Rad, Richmond, CA, USA).

For the binding reactions, 5μg aliquots of nuclear extracts were incubated with probes and 2μg of poly (dI-dC) (Pharmacia Biotech Inc, Uppsala, Sweden) in 20μl of binding buffer (20mmol/L HEPES (pH 7.9), 1mmol/L DTT, 80mmol/L NaCl, 0.2mmol/L EDTA, 0.2mmol/L EGTA, 0.3mmol/L $MgCl_2$, 0.1mmol/L PMSF, 10% glycerol) for 15min at room temperature. The reaction mixtures were then loaded onto 4% non-denaturing polyacrylamide gels in 6.7mmol/L Tris-HCl (pH 7.5), 3.3mmol/L sodium acetate, 1mmol/L EDTA, and 2.5% glycerol. Electrophoresis was performed at 200V in 6.7mmol/L Tris-HCl (pH 7.5), 3.3mmol/L sodium acetate, and 1mmol/L EDTA at 4°C. The gels were dried and subjected to autoradiography. To demonstrate the specificity of DNA–protein binding, the reactions were performed in the presence of non-labeled consensus oligonucleotide competitors. In addition, a supershift assay for AP-1 was carried out using rabbit polyclonal antibodies against Fos or Jun (Santa Cruz Biotechnology) to examine the AP-1 complex containing Fos and Jun. Rabbit polyclonal antibodies against p50-NF-κB or p65-NF-κB (Santa Cruz Biotechnology) were used for the supershift assay in NF-κB. Specific antibodies were added to samples after the initial binding reaction between nuclear protein extracts and ^{32}P-labeled consensus oligonucleotide, and the reaction was incubated at room temperature for 1h.

Table 1 Hemodynamics and Ventricular Weights

	Sham	MI			
		Vehicle	CAN	SPIRO	CAN+SPIRO
Heart rate (beats/min)	248±6	224±2	240±12	237±16	239±7
SBP (mmHg)	123±7††	113±5††	84±5**	103±2††	82±2**
LVEDP (mmHg)	3.3±0.4**	10.9±0.8††	5.6±0.5**,†	8.8±0.8**,††	3.5±0.4**
BW (g)	296±2**	319±6††	301±5**	292±2**	292±4**
LVW (mg/g)	2.23±0.06*,†	2.37±0.05††	2.00±0.04**,†	2.31±0.03††	1.85±0.04**
MI size (%)		35±3	36±3	39±2	36±3

Sham, sham-operated rats; MI, myocardial infarction; SBP, systolic blood pressure; LVEDP, left ventricular end-diastolic pressure; BW, body weight; LVW, left ventricular weight/body weight.
**p<0.05 vs Vehicle, **p<0.01 vs Vehicle, †p<0.05 vs CAN+SPIRO, ††p<0.01 vs CAN+SPIRO. Values are mean±SEM.*

Table 2 Doppler-Echocardiographic Assessment of Left Ventricular Geometry and Function

	Sham	MI			
		Vehicle	CAN	SPIRO	CAN+SPIRO
LVEDd (mm)	8.6±0.2**	10.3±0.2††	9.5±0.2**,†	9.9±0.1*,††	9.0±0.2**
LVEDV (ml)	490±25**	660±15††	566±23**,†	601±15*,††	501±14**
LVEF (%)	58±4**,††	20±1††	30±2**	26±2††	36±2**
E/A ratio	1.8±0.2**,††	5.4±0.4††	3.2±0.4**	4.0±0.5**	3.0±0.3**
E deceleration (m/s²)	1.62±0.08**	2.32±0.08††	2.11±0.15	2.27±0.13††	1.81±0.19**

LVEDd, left ventricular end-diastolic dimension; LVEDV, left ventricular end-diastolic volume; LVEF, left ventricular ejection fraction.
**p<0.05 vs Vehicle, **p<0.01 vs Vehicle, †p<0.05 vs CAN+SPIRO, ††p<0.01 vs CAN+SPIRO. Values are mean±SEM.*

RNA Preparation and Northern Blot Analysis

All procedures were performed as described in detail in our previous reports[9,18] In brief, total RNA was isolated from the septal myocardium by the guanidium thiocyanate–phenol–chloroform method, and 20μg samples of the total RNA were subjected to 1% agarose gel electrophoresis, transferred to nylon membrane, and hybridization was carried out with a (^{32}P)-dCTP-labeled cDNA probe for atrial natriuretic peptide (ANP), brain natriuretic peptide (BNP), collagen type I, collagen type III and glyceraldehyde-3-phosphate dehydrogenase (GAPDH). The densities of an individual mRNA band were measured by a bioimaging analyzer (BAS-2000, Fuji Photo Film, Tokyo, Japan).

Histological and Morphometric Assessments

Four weeks after MI, transverse myocardial sections (5 mm thick) were stained with collagen-specific Sirius red stain. Each field of the non-infarcted myocardium was digitized and then the area of interstitial fibrosis was calculated as the ratio of the sum of the total area of interstitial fibrosis to the sum of the total connective tissue area, and the cardiomyocyte area in all the LV fields of the section. Perivascular areas were not included in this analysis. Average myocyte cross-sectional area was calculated by computer-assisted planimetry.

Statistical Analysis

Results were expressed as mean±SEM. Statistical significance was determined using ANOVA and the Student-Newman-Keuls test. Differences were considered statistically significant at $p<0.05$.

Results

Changes in Hemodynamics and Ventricular Weights

As shown in Table1, there was no significant difference in the size of the MI among the 4 groups. Body weight (BW) was significantly increased in the vehicle group of MI rats ($p<0.01$). In the CAN group and combination group, systolic blood pressure was lower than in the vehicle group ($p<0.01$). LVEDP was significantly higher in the vehicle group than in the sham rats ($p<0.01$). CAN, SPIRO and their combination significantly reduced the increased LVEDP, compared with the vehicle group ($p<0.01$). Moreover, the combination of CAN and SPIRO significantly reduced LVEDP more than that of the CAN group ($p<0.05$) and the SPIRO group ($p<0.01$). LV weight corrected for BW was significantly increased in the vehicle group compared with the sham rats ($p<0.01$). LV weight corrected for BW was significantly lower in the CAN group ($p<0.01$) and combination group ($p<0.01$) compared with the vehicle group. The combination of CAN and SPIRO significantly reduced LV weight, compared with that of the CAN group ($p<0.05$).

Doppler-Echocardiographic Assessment

Echocardiographic assessments of LV geometry and function at 4 weeks are shown in Table2. LVDd and LVEDV were significantly increased in the vehicle rats with MI compared with the sham-operated rats ($p<0.01$). Both the increased LVDd and LVEDV in rats with MI were significantly reduced by CAN or SPIRO. The combination of CAN and SPIRO significantly prevented the increase in LVDd and LVEDV, compared with those of the CAN and SPIRO groups. The vehicle rats with MI had significant systolic dysfunction, as evaluated by decreased LVEF, compared with the sham rats ($p<0.01$). The LVEF in rats with MI was significantly improved by CAN and by the combination therapy. In addition, the combination of CAN and SPIRO significantly improved LVEF, compared with that of the SPIRO group. Furthermore, the vehicle group had significant diastolic dysfunction ($p<0.01$), as defined by an increased ratio of E wave to A wave (E/A ratio) and an E wave deceleration rate (E deceleration),

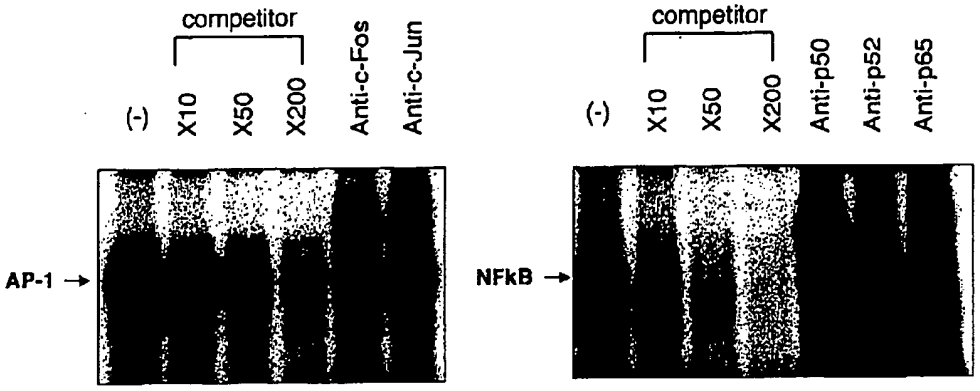

Fig1. Specificity of AP-1 and NF-κB DNA binding activities in the non-infarcted myocardium at 4 weeks after myocardial infarction. A competition assay for AP-1 and NF-κB was carried out in the presence of 10-, 50-, and 200-fold molar excess of unlabelled oligonucleotide (competitor). Supershift analysis was performed with specific anti-c-Fos and anti-c-Jun antibodies for AP-1. Supershift analysis was performed with specific anti-p50 and anti-p65 antibodies for NF-κB.

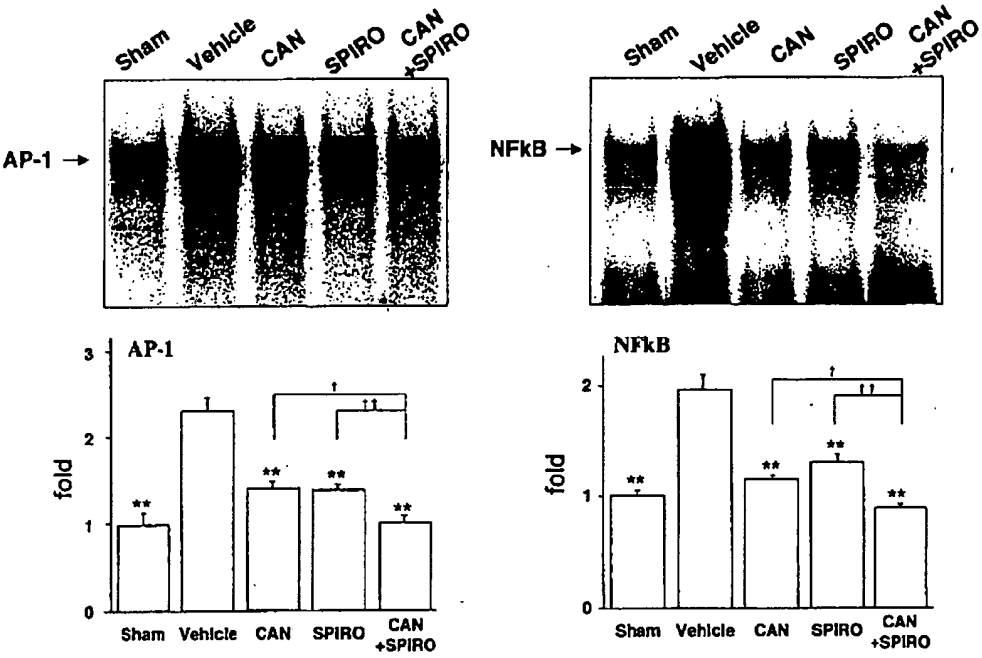

Fig2. Effects of candesartan cilexitil (CAN) and spironolactone (SPIRO) on non-infarcted myocardial AP-1 and NF-κB DNA binding activities at 4 weeks after MI. Myocardial AP-1 and NF-κB DNA binding activities were compared among sham-operated rats (sham) infarcted rats treated with vehicle (MI), infarcted rats treated with CAN, infarcted rats treated with SPIRO and infarcted rats treated with both (CAN+SPIRO). (Upper panels) Representative autoradiogram of gel mobility shift assay of AP-1 and NF-κB DNA binding activities. Each bar represents mean±SEM (n=6). *p<0.05 vs Vehicle, **p<0.01 vs Vehicle. †p<0.05 vs CAN+SPIRO, ††p<0.01 vs CAN+SPIRO. Values are mean±SEM.

compared with the sham group. CAN, SPIRO and their combination significantly improved the E/A ratio ($p<0.01$). E deceleration in the combination therapy group was significantly improved compared with the vehicle and SPIRO groups.

Effects of CAN and SPIRO on Transcriptional Factors and mRNA Expression in Non-Infarcted Myocardium

As shown in Fig 1, the incubation of nuclear protein with ^{32}P-labeled consensus AP-1 or NF-κB oligonucleotide resulted in the formation of one broad band. This shifted band was certified to be specific for AP-1 or NF-κB, because the additional unlabeled consensus oligonucleotide resulted in a decrease in the intensity of the band. The addition of anti-Fos or anti-Jun antibody to the reaction for AP-1 and anti-p50-NF-κB, or anti-p65-NF-κB to the reaction for NF-κB, reduced the intensity of the bands, and these antibodies induced the appearance of supershifted bands.

Table 3 Gene Expression After Myocardial Infarction

	Sham	MI			
		Vehicle	CAN	SPIRO	CAN+SPIRO
ANP	1.00±0.04**	6.62±0.68††	1.99±0.11**,†	3.44±0.22**,††	0.62±0.54**
BNP	1.00±0.08**,†	4.21±2.18††	2.59±0.13**,††	2.18±0.13**,†	1.61±0.03**
Collagen I	1.00±0.13**,†	2.49±0.13††	1.22±0.07**,††	1.25±0.05**,††	0.56±0.07**
Collagen III	1.00±0.12**,††	2.08±0.18††	1.10±0.02**,††	1.23±0.09**,††	0.54±0.05**

ANP, atrial natriuretic peptide; BNP, brain natriuretic peptide.
*p<0.05 vs Vehicle, **p<0.01 vs Vehicle, †p<0.05 vs CAN+SPIRO, ††p<0.01 vs CAN+SPIRO. Values are mean±SEM.

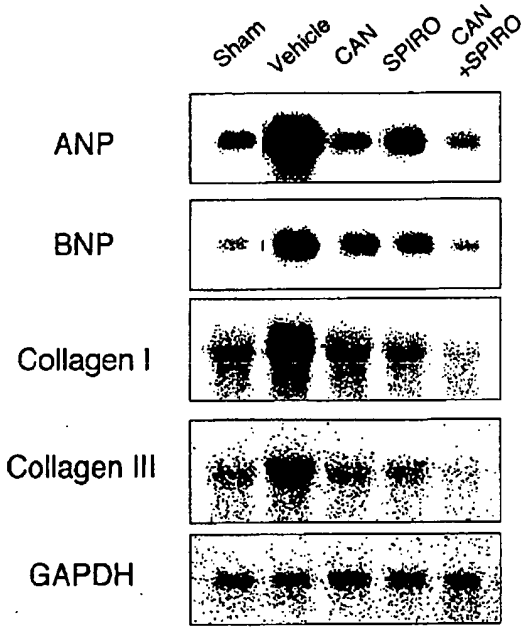

Fig 3. Effects of candesartan cilexitil (CAN) and spironolactone (SPIRO) on non-infarcted myocardial mRNA expression at 4 weeks after MI (n=6 in each group). Myocardial mRNA expression of ANP, BNP, collagen I and collagen III were compared among sham-operated rats (sham) infarcted rats treated with vehicle (MI), infarcted rats treated with CAN, infarcted rats treated with SPIRO and infarcted rats treated with both (CAN+SPIRO). Each panel shows representative autoradiograms from the northern blot analysis of ANP, BNP, collagen I and collagen III.

As shown in Fig 2 and Table 3, MI significantly increased the myocardial transcriptional activity of AP-1 and NF-κB by 2.3- and 2.0-fold, respectively (p<0.01), in the non-infarcted myocardium. CAN and SPIRO inhibited the increase in the DNA binding activity of both AP-1 (61% and 60%, p<0.01) and NF-κB (59% and 66%, p<0.01). The combination of CAN and SPIRO significantly prevented the increase in the transcriptional activities of AP-1 (72% and 73%, p<0.05) and NF-κB (78% and 69%, p<0.05), compared with CAN or SPIRO alone.

The results of cardiac gene expression are shown in Fig 3 and Table 3. The mRNA expression of ANP, BNP and collagen types I and III significantly increased by 6.6-, 4.2-, 2.5- and 2.1-fold, respectively, at 4 weeks after MI (p< 0.01). In the non-infarcted myocardium, CAN and SPIRO significantly attenuated the increased expression of ANP (30% and 51%, p<0.01), BNP (61% and 51%, p<0.01), collagen I (49% and 50%, p<0.01) and collagen III (52% and 59%, p<0.01). Moreover, the combination of CAN and SPIRO reduced the increase in mRNA expression of ANP (31% and 18%, p<0.05), BNP (62% and 73%, p<0.05), collagen I (45% and 44%, p<0.01) and collagen III (49% and 43%, p<0.01) more than either agent alone.

Histomorphometric Findings in Non-Infarcted LV Myocardium

As shown in Fig 4, Sirius red staining revealed a 1.4-fold increase in the cardiac myocyte cross-sectional area (MCSA), a measure of cell hypertrophy, and a 4.3-fold increase in the fraction of interstitial fibrosis in the non-infarcted myocardium compared with the sham-operated rats. The treatments significantly attenuated the cardiomyocyte hypertrophy (CAN: 0.9-fold; SPIRO: 1.0-fold; CAN+SPIRO: 0.9-fold). The fraction of interstitial fibrosis was also prevented by the treatments (CAN: 2.3-fold; SPIRO: 0.8-fold; CAN+SPIRO: 1.1-fold).

Discussion

Accumulating evidence shows that the cardiac renin–angiotensin–aldosterone system (RAAS) is activated during the LV remodeling process that occurs after acute MI[19] Indeed, increased cardiac expression of AT1 receptor, angiotensinogen, Ang II and aldosterone has been reported in the infarcted heart[16,20,21] Silvestre et al showed that the concentration of cardiac Ang II was enhanced in the non-infarcted LV myocardium and that the MI-induced increase in tissue Ang II concentration triggered the rise in cardiac aldosterone production[17] In their model, aldosterone synthase upregulation was abolished by AT1 receptor blockade. Moreover, both mineralocorticoid receptor blockade and AT1 receptor blockade ameliorated fibrosis. A recent study showed that adding SPIRO to the medical treatment for acute MI improved LV chamber dilatation and reduced plasma procollagen after 1 month[22] In the present study, we also observed that CAN and SPIRO reduced the gene expression of collagens I and III, and inhibited myocardial fibrosis in the non-infarcted myocardium. Our findings are consistent with earlier observations that aldosterone is largely responsible for cardiac matrix protein production via a direct effect on the mineralocorticoid receptor[23]

The effect of aldosterone on cardiovascular remodeling has been reported to be different from that of Ang II. Campbell et al found less cardiac inflammation and necrosis in a model of high aldosterone compared with an Ang II infusion model[24] Necrosis induced by Ang II infusion was characterized by macrophages and lymphocytes and neutrophils. Thus, immature scars with fibroblast clusters and interstitial/perivascular fibrosis were observed with Ang II, whereas it is suggested that aldosterone has a direct profi-

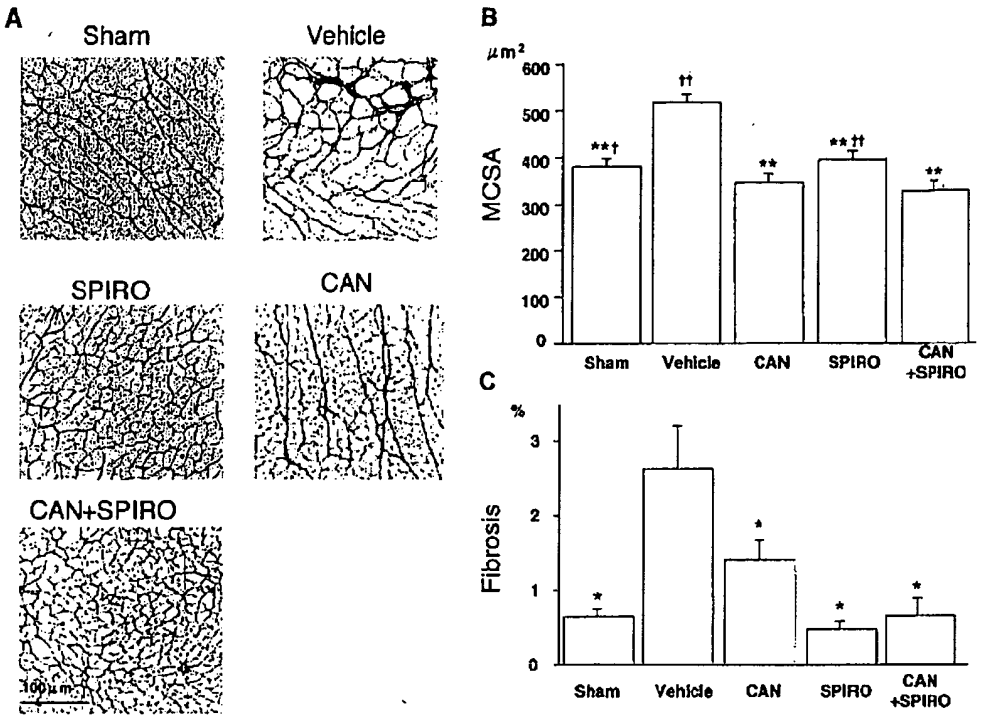

Fig 4. Histopathology of the non-infarcted myocardium of the left ventricle. (A) Photomicrographs show Sirius red-stained cardiac sections from sham-operated rats (sham), infarcted rats treated with vehicle (MI), infarcted rats treated with candesartan cilexitil (CAN), infarcted rats treated with spironolactone (SPIRO) and infarcted rats treated with both drugs (CAN+SPIRO). (B) MCSA, myocyte cross-sectional area; (C) Fibrosis, fraction of interstitial fibrosis. *p<0.05 vs Vehicle, **p<0.01 vs Vehicle. †p<0.05 vs combination, ††p<0.01 vs combination. Values are mean±SEM.

brotic effect. Therefore, the temporal cellular response and appearance of myocardial fibrosis associated with Ang II may be different from those of aldosterone. In our study, although CAN significantly reduced LV weight, SPIRO failed to decrease it. The reason may be the difference in the hemodynamics between CAN and SPIRO. However, both CAN and SPIRO prevented LV dilatation, myocardial fibrosis and cardiomyocyte hypertrophy. Fiebeler et al[25] investigated ARB and SPIRO treatment in rats that were double transgenic for the human renin and angiotensinogen genes, and SPIRO prevented collagen accumulation and cardiac hypertrophy, independent of blood pressure changes. Furthermore, combination therapy with CAN and SPIRO did not change blood pressure compared with CAN alone: however, significantly improved the systolic function and diastolic function. These results suggest that combination therapy with CAN and SPIRO may be better than monotherapy with each, partially independent of hemodynamics, in cardiac remodeling after MI.

Cells respond to extracellular stimuli by activating signal transduction pathways, which cause changes in gene expression. A critical component of a signal transduction pathway is the activation of protein kinases, which phosphorylate cellular substrates regulating the induction of various genes. Previous studies have demonstrated that the numerous growth-associated genes responsible for cardiac remodeling, such as proto-oncogenes, growth factors, contractile proteins or extracellular matrices, are activated in the non-infarcted myocardium after MI, indicating the contribution of altered gene expressions in the process of cardiac remodeling.[26–28] In the present study, we used an electrophoretic mobility shift assay to measured the DNA binding activity of AP-1 and NF-κB as the key transcriptional factors for cell regulation in non-infarcted region during the cardiac remodeling after MI.

Muller et al reported that NF-κB is activated by the Ang II-dependent generation of reactive oxygen species in rats harboring both the human renin and angiotensinogen genes.[29] Tharaux et al showed that the Ang II–related effect on the collagen I gene was mediated via AP-1 in mice expressing the luciferase reporter gene under the control of the promoter of the α2 chain of the collagen I gene.[30] We previously reported that ACEI and ARB could prevent the increase in the activation of non-infarcted myocardial AP-1 and NF-κB after MI in rats![14] Thus, Ang II mediates the activation of both AP-1 and NF-κB in vivo. Moreover, Fiebeler et al[25] demonstrated the activation of myocardial AP-1 and NF-κB in renin and angiotensinogen genes-transgenic rats. They showed that AP-1 activity was markedly reduced, whereas NF-κB activity was only moderately affected by SPIRO treatment compared with that by ARB. Therefore, they speculated that ARB reduced the inflammatory response more effectively than SPIRO. In the present study, SPIRO reduced the increase in the activation of non-infarcted myocardial AP-1 and NF-κB similarly to CAN, and the combination of SPIRO and CAN prevented the activation more than either drug alone, thereby suggesting a synergistic effect on the transcriptional activities. We

also showed that the combination of CAN and SPIRO suppressed the myocardial mRNA expression of ANP, BNP, collagen I and collagen III more effectively than CAN or SPIRO alone. These results suggest there are beneficial effects of combination therapy with CAN and SPIRO on the myocardial cellular response for the prevention of cardiac remodeling after acute MI. However, further work is needed to demonstrate the mechanisms of the difference in myocardial hypertrophy and cardiac fibrosis by treatment with SPIRO or CAN alone.

In conclusion, we demonstrated that in a rat model of MI treatment with the combination of CAN and SPIRO significantly prevented LV remodeling, compared with CAN or SPIRO alone. The combination therapy suppressed the activation of both AP-1 and NF-κB, as well as ANP and BNP gene expressions and collagens, more effectively than CAN or SPIRO alone. These findings suggest that the combination of these 2 agents may be more beneficial than monotherapy for prevention of LV remodeling after MI.

Acknowledgments

This work was supported in part by grants-in-aid for scientific research (Nos 13770356, 14570684 and 15590766) from the Ministry of Education, Science and Culture and a fund for medical research from the Osaka City University Medical Research Foundation. We thank Mihoko Watanabe and Azusa Inagaki for their technical assistance.

References

1. Weisman HF, Bush DE, Mannisi A, Weisfeldt ML, Healy B. Cellular mechanisms of myocardial infarct expansion. *Circulation* 1988; 78: 186–201.
2. Eaton LW, Weiss JL, Bulkley BH, Garrison JB, Weisfeldt ML. Regional cardiac dilatation after acute myocardial infarction: Recognition by two-dimensional echocardiography. *N Engl J Med* 1979; 300: 57–62.
3. Weiss JL, Bulkley BH, Hutchins GM, Mason SJ. Two-dimensional echocardiographic recognition of myocardial injury in man: Comparison with postmortem studies. *Circulation* 1981; 63: 401–408.
4. Pfeffer MA, Braunwald E. Ventricular remodeling after myocardial infarction: Experimental observations and clinical implications. *Circulation* 1990; 81: 1161–1172.
5. Pfeffer MA, Braunwald E, Moye LA, Basta L, Brown EJ Jr, Cuddy TE, et al. Effect of captopril on mortality and morbidity in patients with left ventricular dysfunction after myocardial infarction: Results of the survival and ventricular enlargement trial (The SAVE Investigators). *N Engl J Med* 1992; 327: 669–677.
6. Domanski MJ, Exner DV, Borkowf CB, Geller NL, Rosenberg Y, Pfeffer MA. Effect of angiotensin converting enzyme inhibition on sudden cardiac death in patients following acute myocardial infarction: A meta-analysis of randomized clinical trials. *J Am Coll Cardiol* 1999; 33: 598–604.
7. Cohn JN, Tognoni G. A randomized trial of the angiotensin-receptor blocker valsartan in chronic heart failure. *N Engl J Med* 2001; 345: 1667–1675.
8. Pitt B, Poole-Wilson PA, Segal R, Martinez FA, Dickstein K, Camm AJ, et al. Effect of losartan compared with captopril on mortality in patients with symptomatic heart failure: Randomised trial (the Losartan Heart Failure Survival Study ELITE II). *Lancet* 2000; 355: 1582–1587.
9. Yoshiyama M, Takeuchi K, Omura T, Kim S, Yamagishi H, Toda I, et al. Effects of candesartan and cilazapril on rats with myocardial infarction assessed by echocardiography. *Hypertension* 1999; 33: 961–968.
10. Herzig TC, Jobe SM, Aoki H, Molkentin JD, Cowley AW Jr, Izumo S, et al. Angiotensin II type1a receptor gene expression in the heart: AP-1 and GATA-4 participate in the response to pressure overload. *Proc Natl Acad Sci USA* 1997; 94: 7543–7548.
11. Baeuerle PA, Henkel T. Function and activation of NF-kappa B in the immune system. *Annu Rev Immunol* 1994; 12: 141–179.
12. Guillen I, Blanes M, Gomez-Lechon MJ, Castell JV. Cytokine signaling during myocardial infarction: Sequential appearance of IL-1 beta and IL-6. *Am J Physiol* 1995; 269: R229–R235.
13. Marx N, Neumann FJ, Ott I, Gawaz M, Koch W, Pinkau T, et al. Induction of cytokine expression in leukocytes in acute myocardial infarction. *J Am Coll Cardiol* 1997; 30: 165–170.
14. Yoshiyama M, Omura T, Takeuchi K, Kim S, Shimada K, Yamagishi H, et al. Angiotensin blockade inhibits increased JNKs, AP-1 and NF-kappa B DNA-binding activities in myocardial infarcted rats. *J Mol Cell Cardiol* 2001; 33: 799–810.
15. Zannad F, Alla F, Dousset B, Perez A, Pitt B. Limitation of excessive extracellular matrix turnover may contribute to survival benefit of spironolactone therapy in patients with congestive heart failure: Insights from the randomized aldactone evaluation study (RALES): Rales Investigators. *Circulation* 2000; 102: 2700–2706.
16. Yamagishi H, Kim S, Nishikimi T, Takeuchi K, Takeda T. Contribution of cardiac renin-angiotensin system to ventricular remodelling in myocardial-infarcted rats. *J Mol Cell Cardiol* 1993; 25: 1369–1380.
17. Silvestre JS, Heymes C, Oubenaissa A, Robert V, Aupetit-Faisant B, Carayon A, et al. Activation of cardiac aldosterone production in rat myocardial infarction: Effect of angiotensin II receptor blockade and role in cardiac fibrosis. *Circulation* 1999; 99: 2694–2701.
18. Nakamura Y, Yoshiyama M, Omura T, Yoshida K, Kim S, Takeuchi K, et al. Transmitral inflow pattern assessed by Doppler echocardiography in angiotensin II type 1A receptor knockout mice with myocardial infarction. *Circ J* 2002; 66: 192–196.
19. Patel AR, Konstam MA. Recent advances in the treatment of heart failure. *Circ J* 2002; 66: 117–121.
20. Lindpaintner K, Lu W, Neidermajer N, Schieffer B, Just H, Ganten D, et al. Selective activation of cardiac angiotensinogen gene expression in post-infarction ventricular remodeling in the rat. *J Mol Cell Cardiol* 1993; 25: 133–143.
21. Sun Y, Weber KT. Angiotensin II receptor binding following myocardial infarction in the rat. *Cardiovasc Res* 1994; 28: 1623–1628.
22. Hayashi M, Tsutamoto T, Wada A, Tsutsui T, Ishii C, Ohno K, et al. Immediate administration of mineralocorticoid receptor antagonist spironolactone prevents post-infarct left ventricular remodeling associated with suppression of a marker of myocardial collagen synthesis in patients with first anterior acute myocardial infarction. *Circulation* 2003; 107: 2559–2565.
23. Brilla CG, Rupp H, Funck R, Maisch B. The renin-angiotensin-aldosterone system and myocardial collagen matrix remodelling in congestive heart failure. *Eur Heart J* 1995; 16(Suppl O): 107–109.
24. Campbell SE, Janicki JS, Weber KT. Temporal differences in fibroblast proliferation and phenotype expression in response to chronic administration of angiotensin II or aldosterone. *J Mol Cell Cardiol* 1995; 27: 1545–1560.
25. Fiebeler A, Schmidt F, Muller DN, Park JK, Dechend R, Bieringer M, et al. Mineralocorticoid receptor affects AP-1 and nuclear factor-kappab activation in angiotensin II-induced cardiac injury. *Hypertension* 2001; 37: 787–793.
26. Hanatani A, Yoshiyama M, Kim S, Omura T, Toda I, Akioka K, et al. Inhibition by angiotensin II type 1 receptor antagonist of cardiac phenotypic modulation after myocardial infarction. *J Mol Cell Cardiol* 1995; 27: 1905–1914.
27. Gidh-Jain M, Huang B, Jain P, Gick G, El-Sherif N. Alterations in cardiac gene expression during ventricular remodeling following experimental myocardial infarction. *J Mol Cell Cardiol* 1998; 30: 627–637.
28. Yoshiyama M, Takeuchi K, Hanatani A, Kim S, Omura T, Toda I, et al. Differences in expression of sarcoplasmic reticulum Ca^{2+}-ATPase and Na^{+}-Ca^{2+} exchanger genes between adjacent and remote noninfarcted myocardium after myocardial infarction. *J Mol Cell Cardiol* 1997; 29: 255–264.
29. Muller DN, Dechend R, Mervaala EM, Park JK, Schmidt F, Fiebeler A, et al. NF-kappaB inhibition ameliorates angiotensin II-induced inflammatory damage in rats. *Hypertension* 2000; 35: 193–201.
30. Tharaux PL, Chatziantoniou C, Fakhouri F, Dussaule JC. Angiotensin II activates collagen I gene through a mechanism involving the MAP/ER kinase pathway. *Hypertension* 2000; 36: 330–336.